A Compact Star-Field Sensor for the Los Alamos Designed 1.5U CubeSat System

Hannah D. Mohr, James A. Wren, Nicholas A. Dallmann, Michael C. Proicou, Jerry G. Delapp,
Kimberly K. Katko, John P. Martinez, Donathan J. Ortega, Michael W. Rabin, Daniel N. Seitz,
Paul S. Stein, Justin L. Tripp, Adam Warniment, Robert M. Wheat
Los Alamos National Laboratory
P.O. Box 1663, Los Alamos, NM 87545
hannahm@lanl.gov

ABSTRACT

The Los Alamos National Laboratory (LANL) has designed a compact star-field sensor (SFS) to provide accurate attitude determination to support the pointing requirements of a deployable high-gain antenna on the LANL-designed 1.5U CubeSat platform. The SFS hardware was designed and built entirely at LANL with the goal of minimizing the size requirements and unit costs. Attitude determination is accomplished by comparing the SFS imagery to the Tycho-2 catalog located onboard the satellite. A full "Lost in Space" attitude solution, accurate to about an arcminute, is accomplished in under a minute. The SFS is fully reprogrammable on orbit, allowing continued algorithm development after launch. The first two units were launched in November 2016. We will discuss the hardware design, algorithm development, and field tests.

INTRODUCTION

As CubeSat mission complexity increases, the need for accurate attitude knowledge to assist in attitude control maneuvers becomes more prevalent. The motivation for the design of this star-field sensor (SFS) was to provide accurate attitude information to facilitate proper pointing of a LANL-designed 1.5U CubeSat's high-gain antenna.

A SFS captures an image of the stars within a given field of view (FOV), then compares the pattern of the objects in the image with a catalog of stars stored onboard the satellite. Once the stars in the FOV have been identified, the satellite is able to determine its position based on the known locations of the stars. This approach allows for "Lost in Space" attitude determination, where no *a priori* position knowledge is required for a solution to be found.

The main advantage of a SFS over other types of attitude determination is the precision of the result, which can be within arcminutes of the true solution. A drawback is the time to obtain that solution, since the SFS requires image collection, object extraction, catalog searching, and result verification, causing the known position to lag the current position.

While other SFS have been developed,[1] the goal of this project was to minimize the cost and size of the device to be effective for a 1.5U CubeSat. The main components of the SFS are discussed in the following sections, including the hardware, software, star catalogs, and calibration algorithm.
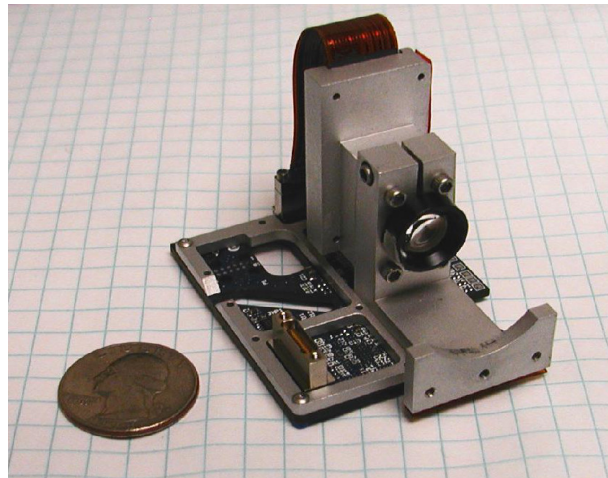
Figure 1: LANL CubeSat Star-Field Sensor Module

HARDWARE DESIGN

The SFS design is based around a Python 1300 image sensor from ON Semiconductor (Figure 2). The sensor is a high-sensitivity monochrome CMOS chip with a 1280 x 1024 pixel array, or 1.3 megapixels (Mpix). Each pixel on the CMOS array has a microlens for improved sensitivity of the individual photodiodes. The Python sensor is mounted on a custom designed circuit board attached to a standard "S-mount" M12 x 0.5 threaded bracket.

Currently the SFS is configured to use the 4300 series 16 mm focal length s-mount lens available from Marshall Electronics, Inc. The lens has 3 elements and a focal ratio of 2.0. The resulting field of view on the

CMOS sensor is 21.7 x 17.5 degrees. The lens is focused before launch using a test target at a distance of approximately 10 meters. The fixture holding the lens is clamped using a set screw and then staked with epoxy before final installation into the spacecraft.
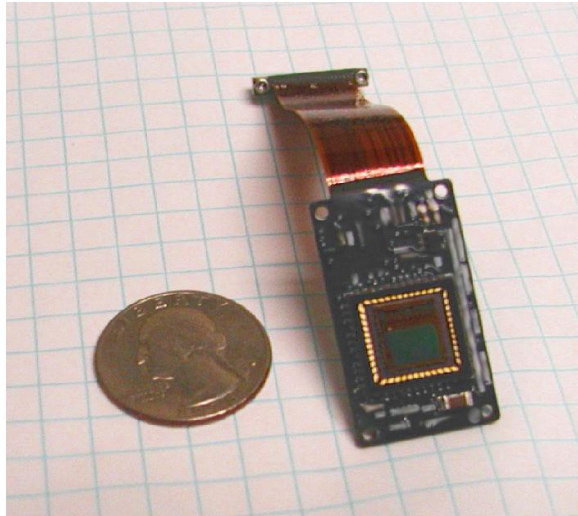

Figure 2: ON Semiconductor Python 1300

The SFS module is controlled by a 32-bit ARM Cortex-M4 processor clocked at 168 MHz with 1 megabyte (MB) of flash memory. The processor is attached to an external SRAM chip providing an additional 8 MB of memory and an external flash chip providing 2 GB of storage. The processor is also paired with a ProASIC A3P1000 Field-Programmable Gate Array (FPGA) from Microsemi that provides the interfaces to the external communication, the interface to the Python sensor, and provides the clocks and power control to the Python sensor. Additionally, the FPGA provides watchdog timers that will reboot the processor if there is a system fault.

The Python sensor is connected to the Digital Camera Interface (DCMI) on the ARM processor which reads the image 10 bits at a time. The image data is transferred to the external SRAM as it is read out. Although the DCMI interface is capable of reading out the CMOS sensor at up to 54 MHz, we were forced to slow the interface down to 2.84 MHz due to reported memory errors when transferring the image to the external SRAM. As a result, full image readout takes about 2.4 seconds.

SOFTWARE DESIGN

The ARM processor runs a real-time operating system (RTOS) provided by ARM's Keil MDK development package (Figure 3). The internal flash memory of the ARM processor is divided into three banks. Bank 0 is 208 MB in size and holds the recovery code which is loaded prior to launch. The Bank 0 code is not intended to be modified after launch and represents the safe recovery mode after a system reset. The other two banks, A and B, are each 384 MB in size and contain the operational flight code which can be updated while on orbit. Code updates are loaded onto Banks A and B in an alternating manner. The system of alternating updates allows easy fallback to the previous version if there is a problem with the most recent code update.
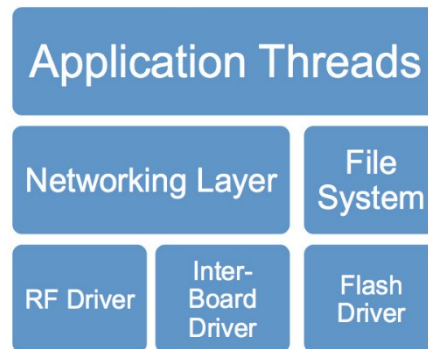

Figure 3: Multi-Threaded

RTOS Architecture

The flight control code is written in the C programming language. The SFS uses a set of code libraries that provide operating system functions, filesystem operations, inter-board communications, and common user interface functions. Additionally we have developed a software library, NavLib, which contains functions for performing common mathematical operations such as linear algebra, orbit determination, astronomical ephemeris, and statistical modeling. The code base is maintained within a Mercurial revision control system.

ATTITUDE DETERMINATION ALGORITHM

The attitude determination algorithm for the SFS takes place in three steps. First, the image is acquired and read into memory. Second, the image is scanned for stars and an object list is produced that provides the image coordinates and brightness in pixel counts of each star that was found. Finally, the extracted object list is calibrated against a known star catalog and the rotation from body to inertial coordinates is determined.

Image Extraction

After an image has been acquired, it must be transformed into a list of stars; a process we call "extraction." The first step in the extraction process is to determine the noise threshold of the image. This is accomplished by finding the median pixel value of a representative portion of the image. We assume this to

be the noise floor of the image and the standard deviation of the noise to be square-root of the noise level. The threshold is then set at 3-sigma above the noise floor.

The next step in the extraction process is to scan the image for sources. As the image is scanned, pixels below the threshold value are discarded. Any pixel above the threshold value is considered a "source" pixel. If a source pixel is adjacent to a pixel from a previously detected source it is added to that source. If the source pixel borders two existing sources, those sources are merged and the pixel is added to the merged source. Finally, if the source pixel does not border a known source, a new one is created. This method of source extraction is expected to handle some image smear due to spacecraft rotation during the image exposure. The level of smear that can be tolerated has yet to be determined via on orbit testing.

For each resulting source, the image coordinates of the centroid are determined using a simple weighted mean.

$$x = \sum (x_i * c_i) / \sum (c_i)$$
$$y = \sum (y_i * c_i) / \sum (c_i)$$
(1)

Where x_i and y_i are the individual pixel coordinates and c_i is the source counts above the image noise floor for that individual pixel.

The resulting object list contains image coordinates for each extracted star as well as the total source counts above the noise level and the number of pixels that the source occupied. The image extraction process currently takes about 6.7 seconds for the full 1.3 Mpix image.

Star Catalog

One of the major software components of the SFS is the star catalogs which provide a reference of known star locations to compare to the objects detected in the camera images.

The primary constraint on the star catalogs was size with a lesser emphasis on how the stars would be sorted since the order can be altered on orbit. Larger catalogs take longer to cycle through, increasing the run time of the algorithm while it searches for the stars captured in the image, while smaller catalogs may not contain sufficient information for the true solution to be included.

A compilation of star catalogs was used, including the Tycho-2 catalog combined with the Tycho-2 Supplement 1 and Yale Bright Star catalogs to ensure a sufficiently large number of stars with the appropriate entry data.[2,3] The brightest stars available were selected to attain the best signal to noise ratio (SNR) and improve the chance they will be observed in the image.

For celestial objects, magnitude of brightness is measured on a negative logarithmic scale, following the relationship

$$M_V = M_{V,1} - M_{V,0} = -2.5 \log(F_1/F_0)$$
(2)

Where M_V is the reported magnitude of the star, $M_{V,1}$ is the overall magnitude, $M_{V,0}$ is the reference magnitude (Vega $\equiv$ 0), F_1 is the observed flux, and F_0 is the reference flux for the optical setup.

Three catalogs were developed to meet different needs of the project:

1. The Complete Catalog, used as a gold standard onboard the satellite, includes all stars with magnitude of brightness (M_V) less than 10.0 and is sorted by ascending magnitude (descending brightness). This catalog includes information about the magnitude, magnitude error, J2000 Equinox position, and proper motion for each of the 362,101 stars, resulting in a binary file size of 7.24 MB. While this catalog is not directly used by the calibration algorithm, the following two catalogs were both generated from the Complete Catalog and any future catalogs can be generated onboard the satellite from this catalog.

2. The Reduced Catalog contains 4,729 stars with positions corrected for proper motion for the epoch of January 1st, 2018. The size of the catalog is reduced to 75.66 kB by including only the magnitude and Cartesian position of each star. The magnitude cutoff for this catalog is 6.0, a selection based on the sensitivity of the optical equipment considering an exposure time of 200 ms. The Reduced Catalog provides indexed star data for look-up by the calibration algorithm once a specific star pair has been selected as a potential match.

3. The Search Catalog enables the calibration algorithm to match potential object pairs to corresponding stars by comparing the spherical distance between vectors. Each entry includes the Reduced Catalog index of two stars and the angle between them. The

magnitude cutoff for this catalog is 5.0 and angle of separation cutoff is 17 degrees, resulting in a catalog size of 24,787 star pairs (297.44 kB).
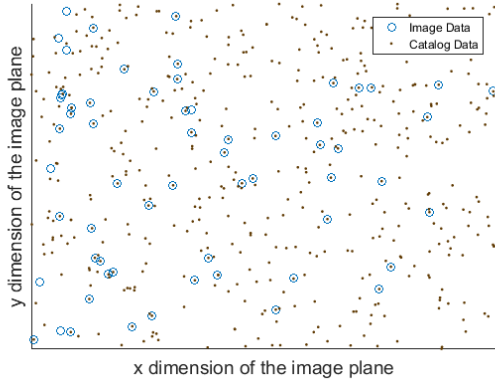

Figure 4: Extracted Image Objects and Catalog Stars

Figure 4 shows the objects extracted from a single SFS image and the catalog stars plotted as they would be seen by the camera for a single exposure. The encircled stars represent catalog matches that can be used for rotation verification in the search algorithm. The image objects that do not encircle a catalog star are counted as misses and reduce the chance that the rotation will be selected. Only catalog stars brighter than magnitude 8 were included in this figure to improve clarity.

Distortion Map

While the optical performance of the lens used for the SFS is very good, it is not perfectly rectilinear. There is a non-uniform radial distortion to the images produced by the optical system that must be corrected before the images are calibrated to the star catalog. We employ a 2 dimensional 3rd order polynomial fit to correct the optical distortions and place the detected objects on a normalized tangential sky projection[4]. Figure 5 shows an exaggerated representation of the distortion effects.
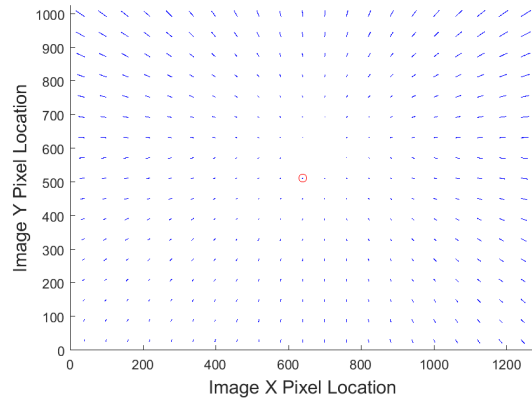

Figure 5: SFS Distortion Map for 16mm Lens (4x Exaggeration)

The optical distortion changes slightly between the different SFS modules. The distortion is dependent on focus, optical alignment, and individual lens characteristics. A generic distortion map is generally adequate to allow successful calibration of the SFS solutions. However, a distortion map that is made specifically for each optical system improves the calibration accuracy and increases the likelihood of a successful match. A camera specific distortion map is made by fitting all of the calibrated objects found in several images to a standard tangential reference plane. Figure 6 shows the fit residuals between catalog and measured stars at the pixel level after distortion correction has been applied.
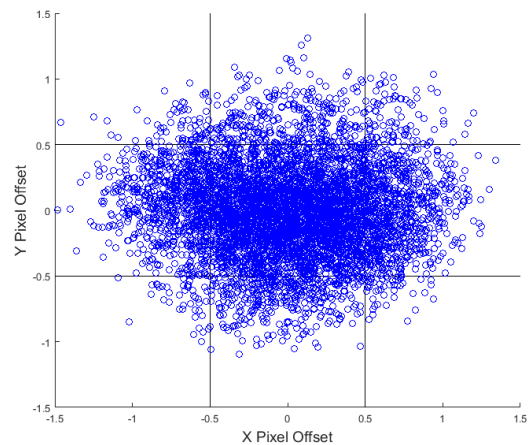

Figure 6: Fit Residuals of the Radial Distortion

The point spread function of the fit residuals was plotted using a probability density function (Figure 7), and the full width at half maximum (FWHM) was computed to determine the error associated with the distortion. FWHM is approximately 0.01884 degrees

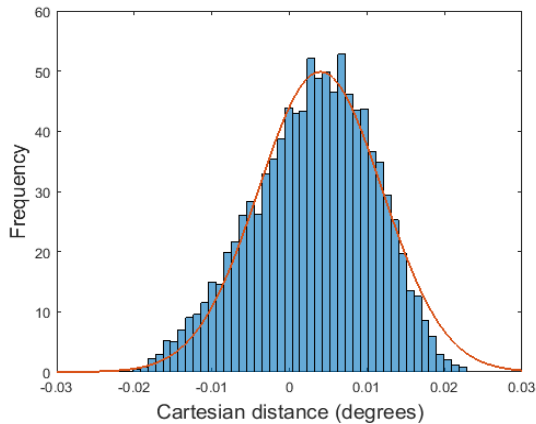(1.10 pixels), indicating the distortion error is about 1.13 arcminutes.

Figure 7: Point Spread Function of Fit Residuals

Image Calibration

While there are several methods which can be used to derive the satellite's attitude from the CMOS sensor image,[5] this research focused on combining TRIAD[6] and Quaternion Estimation (QUEST)[7] algorithms to generate a fast and precise attitude solution. Figure 8 shows a block diagram of the calibration algorithm.
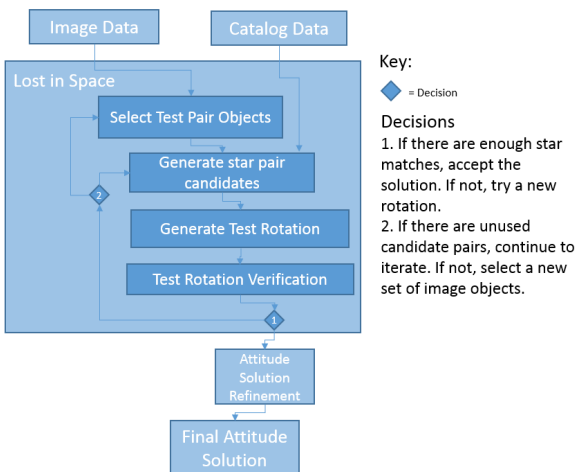

Figure 8: Block Diagram of the Lost-In-Space Calibration Algorithm

The algorithm was designed to meet four main performance characteristics: minimized probability of incorrect result, tolerance to false stars, low probability of inconclusive result, and short time to compute a solution. A description of how the algorithm operates follows.

The objects identified in the image are sorted by brightness using the number of counts recorded by the CMOS sensor; this enables the brightest objects, those with the best SNR, to be tested first. The pair of image objects selected is constrained to be within 13° of the center of the image. False objects not in the catalog, such as planets or hot pixels, are rejected by iterating through object pairs if a solution is not found. The object pair selected at this step is defined to be in SFS body coordinates.

The Search Catalog is used to generate a list of all the star pairs which have nearly the same angle of separation as the selected object test pair. This smaller sub-catalog reduces the search time for each subsequent iteration. A star pair from the candidate list is selected as a potential match to the observed objects.

The initial test rotation is determined with the TRIAD algorithm, which quickly returns a rough conversion from the SFS body coordinates to inertial coordinates. The TRIAD algorithm uses two stars in each coordinate system to find two rotation components that enable a complete mapping of all the stars in the FOV.

In order to verify that the test rotation is correct, it is applied to the remaining stars in the FOV. The rotated stars are then compared to the stars expected to be within the FOV from the Reduced Catalog. If the angle between an image star and the catalog star is less than 0.001 radians, the star is considered a hit. If the rotation has at least 5 hits, the solution is accepted; otherwise, the star pair candidates were incorrect and the function returns to select a new star pair candidate to generate a new test rotation.

Once the rough test rotation has been verified, the QUEST algorithm is applied to the coarse image/catalog star matches to generate a more finely tuned rotation solution. QUEST operates by applying a least squares fit to all the matches to generate the rotation rather than using only two stars, thereby including more of the image information in the attitude solution.

The resulting attitude solution is saved and used in the next SFS measurement to select the correct stars from the catalog at the beginning of the calibration, significantly improving the calibration time.

FIELD TESTS

The camera hardware was tested at LANL's Fenton Hill Observatory by capturing 277 images of stars using exposure times ranging from 200 ms to 1000 ms. The object extraction algorithm was performed (Figure 9),

generating files which were read by the calibration algorithm.

Algorithm solutions were confirmed with known star patterns based on the time and location the images were collected. The goals of the field tests were to investigate the properties of the optical setup and verify the attitude determination algorithm could effectively interpret the information collected by the SFS camera. The algorithm was developed in Matlab; initial testing was performed on the development version followed by testing of the flight version on the ARM processor.
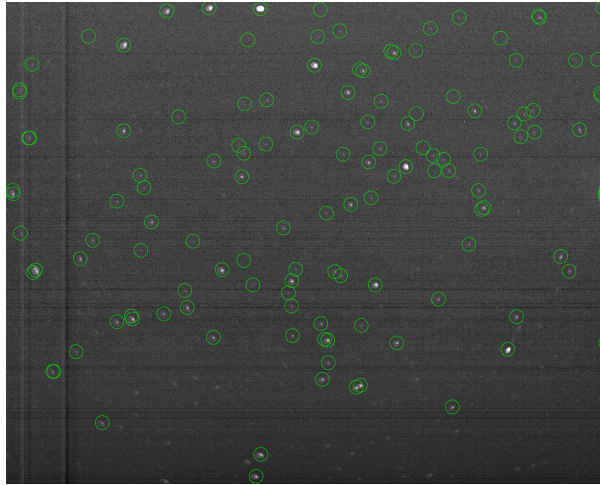

Figure 9: 1s SFS Exposure with Extracted Stars Circled in Green

The sensitivity of the optical equipment was investigated by observing the quality of the objects at varying exposure times based on the error measurements provided by *Astrometry.net,*[8] an online resource used by astronomers to identify star images and obtain detailed astrometric information about the stars therein. The magnitude error versus magnitude plot (Figure 10) provides the mathematical relationship between brightness of an object and quality of the measurement. The exposure time of the image changes the SNR of an object at a given magnitude, as seen in the horizontal shift in the trend.

The desired sensitivity of the optical equipment was determined based on a SNR of 5-sigma, which corresponds to the 0.2 magnitude error line in Figure 10. It was observed that stars with magnitude greater than 10 had such high error that they were insignificant. This was a leading consideration in the magnitude cutoff for the Complete Catalog.
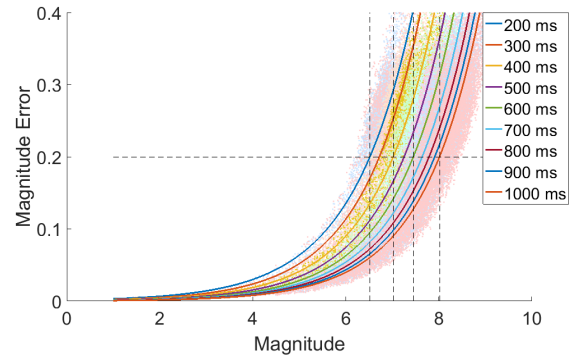

Figure 10: Error of Magnitude Measurement at Varying Exposure Times

A second test to investigate sensitivity was to determine the approximate magnitude at which the sensor was unable to detect stars at a given exposure time. The number of stars observed increases with decreasing brightness until the baseline noise level begins to dominate, at which point there is a steep decline in observed stars. The peaks in Figure 11 show the cutoff for the observable star magnitude at exposure times ranging from 200 ms to 1000 ms.
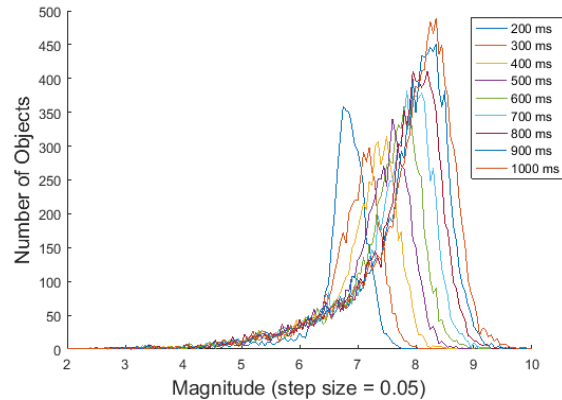

Figure 11: Objects in FOV at a Given Exposure

The average number of objects detected in a FOV was plotted to determine if a sufficient number were available to solve the star field. Figure 12 shows that the shortest exposure time still had, on average, more than 50 objects brighter than the magnitude cutoff in the field of view, a large enough number to successfully apply the calibration algorithm.
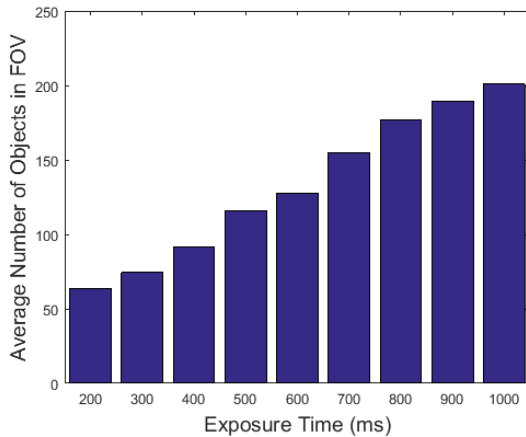
Figure 12: Average Number of Objects in FOV at Different Exposure Times

Algorithm Error Analysis

Two types of errors were investigated: incorrect results, which occur when the algorithm provides a solution with an angle of error greater than 60 arcminutes (1 degree); and inconclusive results, indicating the algorithm was unable to identify any solution for the image.

The images collected by the SFS camera were analyzed using *Astrometry.net* to generate a precise attitude solution independent from the SFS calculations. The accuracy of each SFS solution was measured by calculating the angle between the computed attitude solution and the reference solution. Table 1 summarizes the error measurements for the 200 ms exposure images and the complete list of images. The average error was less than an arcminute and the maximum error was within 60 arcminutes, indicating that no incorrect results were obtained.

Table 1: Summary of Attitude Solution Errors

	200 ms Exposures	All Exposures
Mean Error	0.9273 arcmin	0.6266 arcmin
Minimum Error	0.0885 arcmin	0.0205 arcmin
Maximum Error	6.3040 arcmin	17.3349 arcmin

During the Matlab test of all 277 images, the algorithm was able to find a solution for each case; no inconclusive results were recorded.

SFS Solution Speed

The time required to obtain an attitude solution depends on several components within the SFS, including image collection with the optics, image extraction to obtain a list of objects, and calibration of the image to solve for the attitude quaternion.

The image collection time varied with exposure time, ranging from 200 ms to 1000 ms during the field tests. Reading the image took about 2.4 seconds, and image extraction took approximately 6.7 seconds when tested on the ARM processor.

The calibration time was recorded for both the Matlab development version and the ARM processor version. In Matlab, the time from when the image data was read in to when the attitude solution was available was recorded to be 175 ms on average for the 277 test images. For more than 50% of the cases, the algorithm selected the correct star pair as its initial choice, improving the average run time for those cases to under 30 ms. On the ARM processor, calibration time varied from 2.7 s to 56 s.

When the SFS had a previous attitude solution available which it could use as a reference, the calibration time was significantly reduced because catalog searching was minimized. On the ARM processor, the calibration algorithm took less than a second to determine the updated attitude solution from a previous known position.

ON ORBIT RESULTS

The first two Los Alamos Designed CubeSats that contained SFS modules were launched in November of 2016. The launch and deployment of the satellites was successful and ground communication has been established with both satellites. Technical challenges with the radio communication and power systems are currently being addressed with on orbit software updates. As a result, testing of the SFS system has been limited to date. On orbit testing of the SFS system is planned for the summer of 2017.

FUTURE IMPROVEMENTS

The calibration algorithm has been ported to the ARM microprocessor and successfully tested on the archival SFS test images from the Fenton Hill observatory. After initial on orbit testing of the SFS system, it will be integrated into the ADCS control loop as a supplement to the sun-vector and magnetometer attitude sensors.

The primary area of interest for future design work is improving the calibration speed. Image extraction time could be reduced by saving the previous extraction information so the pixels which are most likely to include stars could be read first. Improvements to the calibration algorithm will continue to be investigated,

including developing more advanced catalog search techniques based on magnitude so false stars can be rejected more rapidly, or enabling angle look-up functionality within the catalogs to reduce the search time.

Another way to reduce the lag between the current attitude and the computed attitude is to combine the SFS data with gyro data, forming a gyro-stellar estimation.[9] This would enable the attitude solution produced by the SFS to be updated by the high-frequency gyro sensors while the new SFS solution was being generated.

CONCLUSIONS

The result of this research was the development and testing of a star-field sensor which has been shown in field tests to successfully identify its attitude without *a priori* position knowledge. The hardware and star catalogs have been deployed onto two 1.5U CubeSats, while the calibration algorithm is waiting to be uploaded.

The field tests show that the SFS can produce the rotation representing the current attitude within an arcminute of the true solution. With continued development, this SFS will be applicable to future 1.5U CubeSat platforms.

REFERENCES

1. M. S. Scholl. "Star-Field Identification for Autonomous Attitude Determination", Journal of Guidance, Control, and Dynamics, vol. 18, No. 1, 1995.

2. Pickles, A.J., "A Stellar Spectral Flux Library: 1150 – 25000 Å," Publications of the Astronomical Society of the Pacific, vol. 110, No. 749, 1998.

3. Hoffleit, D., C. Jaschek, "The bright star catalogue," The Bright Star Catalogue, New Haven: Yale University Observatory (4th Edition), 1982.

4. Shupe, L.D., M. Moshir, L. Jing, R. Narron, "The SIP Convention for Representing Distortion in FITS Image Headers," Astronomical Data Analysis Software and Systems XVI, vol. 347, 2005.

5. Spratling, B.B. and D. Mortari, "A Survey on Star Identification Algorithms," Algorithms, vol. 2, No. 1, January 2009.

6. Bar-Itzhack, I.Y., R.R. Harman, "Optimized TRIAD algorithm for attitude determination," Journal of guidance, control, and dynamics, vol. 20, No. 1, 1997.

7. Shuster, M. D., Oh, S. D., "Three-Axis Atttitude Determination from Vector Observations," Journal of Guidance, Control, and Dynamics, vol. 4, No. 1, 1981.

8. Lang, D., Hogg, D. W., Mierle, K., Blanton, M., & Roweis, S., "Astrometry.net: Blind Astrometric Calibration of Arbitrary Astronomical Images," The Astronomical Journal, vol. 139, 2010.

9. Winkler, S., "Observability of Star Tracker/Gyro Based Attitude Estimation Considering Time-Variant Sensor Misalignment," Advances in Aerospace Guidance, Navigation and Control, 2011.